

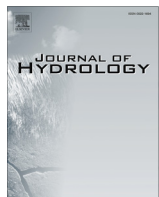


ELSEVIER

Contents lists available at ScienceDirect

Journal of Hydrology

journal homepage: www.elsevier.com/locate/jhydrol



Research papers

Assessing the ability of potential evapotranspiration models in capturing dynamics of evaporative demand across various biomes and climatic regimes with ChinaFLUX measurements



Han Zheng ^{a,b}, Guirui Yu ^{b,g,*}, Qiu Feng Wang ^{b,g}, Xianjin Zhu ^{a,c}, Junhua Yan ^d, Huimin Wang ^b, Peili Shi ^b, Fenghua Zhao ^b, Yingnian Li ^e, Liang Zhao ^e, Junhui Zhang ^f, Yanfen Wang ^g

^a State Key Laboratory of Loess and Quaternary Geology, Institute of Earth Environment, Chinese Academy of Sciences, Xi'an 710061, China

^b Key Laboratory of Ecosystem Network Observation and Modeling, Institute of Geographic Sciences and Natural Resources Research, Chinese Academy of Sciences, Beijing 100101, China

^c College of Agronomy, Shenyang Agricultural University, Shenyang 110161, China

^d South China Botanical Garden, Chinese Academy of Sciences, Guangzhou 510650, China

^e Northwest Institute of Plateau Biology, Chinese Academy of Sciences, Xining 810001, China

^f Institute of Applied Ecology, Chinese Academy of Sciences, Shenyang 110016, China

^g College of Resources and Environment, University of Chinese Academy of Sciences, Beijing 100049, China

ARTICLE INFO

Article history:

Received 5 December 2016

Received in revised form 26 May 2017

Accepted 27 May 2017

Available online 29 May 2017

Keywords:

Evaporative demand

Potential evapotranspiration

Actual evapotranspiration

Penman

Priestly-Taylor

Linacre

ABSTRACT

Estimates of atmospheric evaporative demand have been widely required for a variety of hydrological analyses, with potential evapotranspiration (PET) being an important measure representing evaporative demand of actual vegetated surfaces under given metrological conditions. In this study, we assessed the ability of various PET models in capturing long-term (typically 2003–2011) dynamics of evaporative demand at eight ecosystems across various biomes and climatic regimes in China. Prior to assessing PET dynamics, we first examined the reasonability of fourteen PET models in representing the magnitudes of evaporative demand using eddy-covariance actual evapotranspiration (AET) as an indicator. Results showed that the robustness of the fourteen PET models differed somewhat across the sites, and only three PET models could produce reasonable magnitudes of evaporative demand (i.e., $\text{PET} \geq \text{AET}$ on average) for all eight sites, including the: (i) Penman; (ii) Priestly-Taylor and (iii) Linacre models. Then, we assessed the ability of these three PET models in capturing dynamics of evaporative demand by comparing the annual and seasonal trends in PET against the equivalent trends in AET and precipitation (P) for particular sites. Results indicated that nearly all the three PET models could faithfully reproduce the dynamics in evaporative demand for the energy-limited conditions at both annual and seasonal scales, while only the Penman and Linacre models could represent dynamics in evaporative demand for the water-limited conditions. However, the Linacre model was unable to reproduce the seasonal switches between water- and energy-limited states for some sites. Our findings demonstrated that the choice of PET models would be essential for the evaporative demand analyses and other related hydrological analyses at different temporal and spatial scales.

© 2017 Elsevier B.V. All rights reserved.

1. Introduction

Changes in global hydrological cycle could lead to major environmental and socioeconomic impacts (Oki and Kanae, 2006), while estimates of atmospheric evaporative demand is widely required for hydrological analyses such as irrigation scheduling,

water resources management, drought monitoring and hydroclimatologic variability (Allen et al., 1998; Budyko, 1978; Hobbins et al., 2012; Liu and Sun, 2016; Roderick and Farquhar, 2004; Wang et al., 2012). Atmospheric evaporative demand can be expressed in different perceptions, such as pan evaporation from an open-water surface, reference evapotranspiration from a well-watered but prescribed reference vegetated surface with a fixed surface resistance (e.g., Allen et al., 1998; crop reference evapotranspiration), and potential evapotranspiration (PET) from a hypothetically well-watered but actual vegetated surface

* Corresponding author at: 11A Datun Road, Chaoyang District, Beijing 100101, China.

E-mail address: yugr@igsnrr.ac.cn (G. Yu).

(Robinson et al., 2017), thereby making PET the most suitable measure representing evaporative demand of actual land surfaces under given metrological conditions. PET could be estimated by some physical or empirical models (Federer et al., 1996; Fisher et al., 2011). However, numerous PET models have been introduced in the literature (Fisher et al., 2011; Rao et al., 2011), and there may exist significant differences among their estimates and variation trends (e.g., Donohue et al., 2010; Federer et al., 1996; Fisher et al., 2005, 2011). Therefore, it is necessary for us to determine the appropriate PET model(s) representing evaporative demand, especially for analyses on long-term dynamics in evaporative demand under global climate change.

The concept of water-limited and energy-limited evaporation was applied to assess the ability of PET models in representing evaporative demand in this study. These two terms have long been used for understanding the role of evaporation in the water balance at various space-time scales (McVicar et al., 2012a). The hydroclimatological term 'energy-limited' is used to describe the conditions when the supply of water exceeds the evaporative demand, while the term 'water-limited' refers to the contrary circumstances (Donohue et al., 2010; McVicar et al., 2012a). Generally, we would expect actual evapotranspiration (AET) to approach PET under energy-limited environments where AET is mainly determined by PET, i.e., the proportional relationship (Roderick and Farquhar, 2004). As for water-limited conditions, AET will increase with increases in precipitation (P) due to more surface moisture availability, while PET will decrease because of the associated decreases in solar radiation and air temperature, and increases in air humidity (Donohue et al., 2010; Roderick and Farquhar, 2004; Yang et al., 2006). That is, for water-limited conditions, the relationship between PET and AET (and also P) should generally follow an inverse relationship, i.e., the complimentary relationship (Brutsaert and Parlange, 1998; Yang et al., 2006).

It seems quite easy for us to portray the 'realistic' long-term trends in PET and hence evaporative demand according to AET or P trends if we are certain about the studied locations or periods under either water- or energy-limited environments. For example, Donohue et al. (2010) utilized the logic of complimentary relationship to assess if there is an inverse relationship between P trends and PET trends as a means to assess the usefulness of different PET formulations in capturing dynamics in evaporative demand for water-limited locations. However, as a matter of fact, we are not definitely sure about the water- or energy-limited states for many situations but only with some empirical knowledge (mainly from the long-term average ratio of PET rates to P rates (Donohue et al., 2007), but PET data source is inconclusive). It becomes more difficult for the 'equitant' climates, that is, the condition straddles the divide between water- and energy-limited states and the dominant limitation switches between these states at a time-step shorter than mean-annual (e.g., seasonally) (McVicar et al., 2012b). Therefore, it is necessary to find a feasible way to define the water- or energy-limited states in order to evaluate the capability of PET models in capturing dynamics in evaporative demand.

Based on the logic of proportional and complimentary relationship between AET and PET, it should be noted that there also exist proportional or inverse relationships between AET trends and P trends for different hydroclimatological conditions (i.e., water- or energy-limited), which have been observed in previous studies (e.g., Brümmer et al., 2012; Song et al., 2014). That is, the relationship between the trends of AET and P should be proportional for the water-limited conditions, while inverse relationship would be expected for the energy-limited (not water-limited) environments. Thus, it is executable for us to define the hydroclimatological states according to the observed relationships between AET trends and P

trends, and hence obtain the 'realistic' equivalent trends in PET and evaporative demand.

Therefore, this study aims to assess the utility of fourteen PET models in capturing annual and seasonal dynamics of evaporative demand, using the observed relationship between the trends of AET and P as an approach to define the corresponding hydroclimatological (i.e., water- or energy-limited) states. In consideration of the significant differences among different PET model estimates, validating the reasonability of PET estimates in representing the magnitudes of evaporative demand should be an important initial step when assessing the ability of PET models in capturing dynamics in evaporative demand.

To accomplish this, three objectives are proposed in this research: (i) assessing the magnitudes of PET; (ii) assessing the annual trends of PET; and (iii) assessing the per-month trends of PET. This paper is organized in the following sections. In the next section 'Materials and Methods' we describe: (i) the sites used in this study; (ii) the measurements and data processing of AET and meteorological data used for these analyses; (ii) the PET models selected in this research; (iii) the assessment on PET magnitudes; and (iv) the assessment on PET dynamics. The section 'Results' are presented using sub-headings the same with the three objectives. A discussion on the magnitudes and dynamics of PET are displayed next, followed by some conclusion.

2. Materials and methods

2.1. Site description

AET measurements and meteorological data used in this study were collected from eight typical ecosystems with eddy-covariance flux towers, as part of ChinaFLUX (Yu et al., 2006). The eight sites consisted of three forest sites, three grassland sites, one wetland site and one cropland site. The three forest sites are distributed from north to south in the eastern China, containing a temperate broadleaf Korean pine mixed forest in the Changbai Mountains (CBS), a subtropical coniferous plantation in the Qianyanzhou site (QYZ), and a subtropical evergreen broadleaf forest in the Dinghu Mountains (DHS). They are influenced by monsoon climate to varying degrees and expand from temperate zone to subtropical zone (Yu et al., 2006). The three grassland sites and the wetland site are located in the North of China and the Qinghai-Tibet Plateau, containing a typical temperate steppe in Inner Mongolia site (NM), an alpine shrubland meadow in Haibei site (HBGC), an alpine marsh meadow in Haibei site (HBSD, we considered it as a wetland site in this study), and an alpine meadow-steppe in Dangxiong site (DX). The cropland site is Yucheng site (YC) locating in the Northern China Plains, which is a typical temperate cropland with annual rotation of winter wheat and summer maize in China. These eight sites are separated along a broad geographical distribution and encompass the most prevalent climate and ecosystem types in China (Fig. 1), spanning wide ranges of temperature and precipitation. An overview of the site characteristics is given in Table 1. More extensive descriptions could be found in the references listed in Table 1.

2.2. AET and meteorological data

AET data were acquired from water flux data directly measured by eddy covariance method. CO_2 and H_2O flux data were measured by the open-path eddy covariance (OPEC) system above the canopy at the ChinaFLUX sites. The OPEC system consisted of an open-path infrared gas analyser (Model LI-7500; Licor Inc., Lincoln, Nebraska, USA) and a 3-D sonic anemometer (Model CSAT3; Campbell

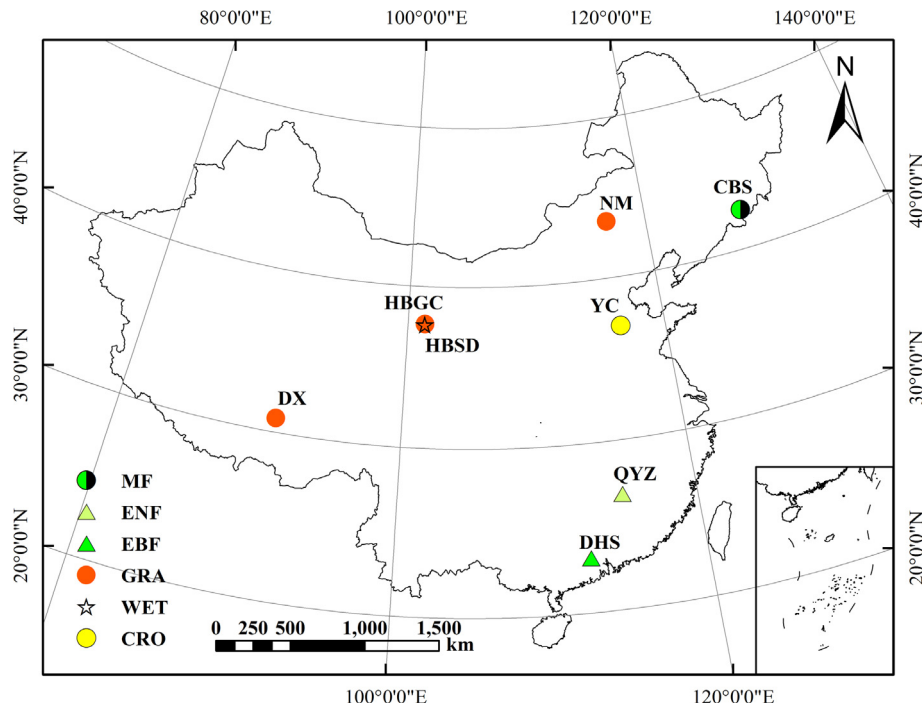


Fig. 1. Location of the eight eddy covariance flux sites used in this study. Different marker types indicate different vegetation types: MF, mixed forests; ENF, evergreen needleleaf forests; EBF, evergreen broadleaf forests; GRA, grasslands; WET, wetlands; CRO, croplands.

Table 1
Site descriptions of the eight sites.

Sites	CBS	QYZ	DHS	NM	HBGC	HBSD	DX	YC
Location	42.40°N, 128.10°E	26.74°N, 115.06°E	23.17°N, 112.57°E	43.55°N, 116.68°E	37.66°N, 101.33°E	37.61°N, 101.31°E	30.85°N, 91.08°E	36.95°N, 116.57°E
Elevation (m)	738	102	300	1200	3293	3160	4333	28
Temperature (°C) ^a	3.6	17.9	20.8	-0.4	-1.6	-1.6	1.3	13.1
Precipitation (mm) ^b	695.3	1494	1956	350.4	560	560	476.8	528
Climate type	Temperate continental monsoon climate	Typical subtropical monsoon humid climate	South-subtropical monsoon humid climate	Temperate semi-arid continental climate	Plateau continental climate	Plateau continental climate	Plateau monsoon climate	Temperate semi-humid monsoon climate
Vegetation type ^b	Temperate broadleaf Korean pine mixed forest (MF)	Coniferous plantation (ENF)	Evergreen broadleaf forest (EBF)	Typical temperate steppe (GRA)	Alpine shrubland meadow (GRA)	Alpine swamp meadow (WET)	Alpine meadow-steppe (GRA)	Warmer temperate dry farming cropland (CRO)
Dominant species	<i>Pinus koraiensis</i> , <i>Tilia amurensis</i> , <i>Quercus mongolica</i>	<i>Pinus massoniana</i> , <i>Pinus elliottii</i> , <i>Cunninghamia lanceolata</i>	<i>Schima superba</i> , <i>Castanopsis chinensis</i> , <i>Pinus massoniana</i>	<i>Agropyron cristatum</i> , <i>Cleistogenes squarrosa</i> , <i>Carex duriuscula</i>	<i>Dasiphora fruticosa</i>	<i>Kobresia tibetica</i>	<i>Kobresia pygmaea</i> , <i>Stipa capillacea</i> , <i>Carex montis</i>	<i>Triticum aestivum</i> , <i>Zea mays</i>
Canopy height (m)	26	12	20	0.4	0.6	0.5	0.15	0.8(wheat) (maize)
LAI (m ² m ⁻²) ^c	1.45	3.68	3.2	0.45	0.79	0.89	0.15	0.86
Duration Reference	2003–2010 (Zhang et al., 2006)	2003–2011 (Wen et al. (2006))	2003–2010 (Yu et al. (2006))	2004–2011 (Hao et al. (2007))	2003–2011 (Zheng et al. (2014))	2004–2010 (Yu et al. (2006))	2004–2010 (Shi et al., 2006)	2003–2011 (Zhao et al., 2007)

^a They are mean annual temperature and mean annual precipitation for recent 20 to 30 years, respectively.

^b The abbreviations in the brackets are IGBP (International Geosphere-Biosphere Program) vegetation types: MF, mixed forests; ENF, evergreen needleleaf forests; EBF, evergreen broadleaf forests; GRA, grasslands; CRO, croplands; WET, wetlands.

^c LAI here is the mean leaf area index for each site in 2004, which was estimated from a MODIS LAI product (MOD15A2) with a temporal resolution of 8 days and a spatial resolution of 1 km ORNL DAAC (2015).

Scientific Inc., Logan, Utah, USA). All signals were sampled with a frequency of 10 Hz and then calculated and recorded with a data logger (Model CR5000, Campbell Scientific Inc., Logan, Utah, USA) at half-hour intervals. The meteorological variables including but

not limited to solar radiation, air temperature, precipitation, wind speed and relative humidity were synchronously obtained with a frequency of 2 s and block averaging over 30 min as well, in which precipitation data were measured using a tipping-bucket rain

gauge. Further details about monitoring systems could be found in Yu et al. (2006) and Yu et al. (2013).

To guarantee the flux data quality, a series of processing procedures recommended by ChinaFLUX were applied to the raw 30-min flux data (Yu et al., 2006). Firstly, three-dimensional rotation method was applied to the wind components to make the average vertical wind speed to zero and to force horizontal wind to the mean wind direction (Finnigan et al., 2003; Zhu et al., 2005). Then we used Webb-Pearman-Leuning (WPL) correction method to adjust the effects of density change on CO₂ and H₂O fluxes (Webb et al., 1980). We calculated the storage terms of water fluxes, and removed the spurious data from the dataset later. The spurious data were defined mainly by four criteria, i.e., (i) data recorded during and half hour before and after precipitation events; (ii) latent heat flux data out the threshold of [-100, 500] (w m⁻²); (iii) 1.96 times standard deviation principle; and (iv) friction velocity (u^*) threshold which was calculated according to Reichstein et al. (2005). Then data gaps in the water flux data were filled with a look-up table method (Reichstein et al., 2005). At last, daily (i.e., 24-h) AET value was calculated by summing 30-min values. Monthly and annually AET were then accumulated from daily and monthly AET observations, respectively. All the data processing procedures mentioned above were performed with a Matlab program written in-house. See Yu et al. (2006) for more information about the data quality control and gap filling.

2.3. Selected PET models

Fourteen PET models were selected in this study, containing one fully physically based method, six radiation-based models and seven temperature-based models (Table 2). These models were selected because they represent a range in how the key input variables (e.g., solar radiation, air temperature, vapor pressure, and wind speed) are treated. The selected models varied from the fully physical Penman equation with four variables to the empirical Thornthwaite model that contains only one meteorological variable (i.e., air temperature). The fourteen PET models are briefly presented in Table 2, while their formulae are listed in the Appendix in detail. All these PET methods used observed daily meteorological data above the canopy for each site as inputs, which were synchronously obtained with ecosystem-scale flux data.

Except that Thornthwaite model (Thornthwaite, 1948) and Kharrufa model (Xu and Singh, 2002) were designed against monthly scale, the other twelve models directly estimated daily PET values. Monthly and annually PET were accumulated from

daily and monthly PET estimates, respectively. The mean daily PET values for the Thornthwaite and Kharrufa models were calculated by dividing their total PET values by total days during the observational periods (Table 1), respectively. In addition, negative PET estimates were set as zero in this study.

2.4. Assessment on PET magnitudes

Before testing the ability of PET models in capturing dynamics of evaporative demand, we first assessed the reasonability of PET estimates in representing the magnitudes of evaporative demand. Towards this end, the key issue is to set the standard for electing the 'reasonable' PET model(s). Conceptually, PET represents the upper limit of AET (Thornthwaite, 1948). Hence, AET should never exceed PET at a long-term scale (e.g., annual time step) (Fisher et al., 2011), which hence makes AET a straight-forward and objective indicator for the 'reasonability' validation of PET models.

Thus, when assessing the PET magnitudes, we compared the daily average PET estimates of the fourteen PET models (Table 2) with the equivalent rates of observed site-based AET data over the eight ecosystems in China, to determine whether each of them could give reasonable PET estimates (i.e., PET ≥ AET on average). Moreover, one-way analysis of variance and Tukey's multiple comparison tests were applied to determine the differences among the selected PET models at the daily time scale. The differences were considered to be significant if p -values are smaller than 0.05.

2.5. Assessment on PET dynamics

According to the results from the assessment on the PET magnitudes, several PET models were identified as reasonable to calculate PET values for all the eight sites. Then, these PET models were further used to test their ability in representing annual and seasonal dynamics of evaporative demand. Here, we analyzed the annual and seasonal trends of each PET model estimates, respectively, and comparing them against the equivalent trends in AET and precipitation (P) for particular sites. For a given site, PET dynamics were determined using the same method as Donohue et al. (2010). That is, we calculated the linear trends of PET rates for each month over the observational periods (Table 1) with the method of ordinary least square regression. Since the units of monthly PET data are mm mth⁻¹, the corresponding units for annual trends in these monthly data (i.e., the slope values of the regression lines with x -axis as years) should be mm mth⁻¹ yr⁻¹. Annual trends in PET were calculated as the sum of twelve monthly

Table 2
PET models selected for this study.

Classification	No.	Common model name	Input variables	Reference
Fully physical	1	Penman	R_n, T_a, e_a, u	Penman (1948)
Radiation-based	2	Makkink	R_s, T_a	Xu and Singh (2002)
	3	Turc	R_s, T_a, RH	Lu et al. (2005)
	4	Jensen-Haise	R_s, T_a	Jensen and Haise (1963)
	5	Stephens-Stewart	R_s, T_a	McGuinness and Bordne (1972)
	6	Priestly-Taylor	R_n, T_a	Priestley and Taylor (1972)
	7	Hargreaves	R_s, T_a	Hargreaves (1975), Xu and Singh (2000)
Temperature-based	8	Blaney-Criddle	T_a, p	Xu and Singh (2002)
	9	Romanenko	T_a, e_a	Romanenko (1961)
	10	Hamon	T_a, L_{day}	Hamon (1960), Oudin et al. (2005)
	11	Linacre	T_a, T_d	Linacre (1977)
	12	Hargreaves-Samani	$T_a, T_{max}, T_{min}, R_a$	Hargreaves and Samani (1982)
	13	Thornthwaite ^a	T_a, L_{day}	Thornthwaite (1948)
	14	Kharrufa ^a	T_a, p	Xu and Singh (2001)

R_n , net radiation; T_a , mean air temperature; T_{max} and T_{min} , maximum and minimum air temperature, respectively; VPD, vapor pressure deficit; e_a , actual vapor pressure; u , wind speed; R_s , incident solar radiation; RH, relative humidity; L_{day} , maximum possible duration of sunlight or daylight hours; p , daily percentage of total annual daytime hours; R_a , extraterrestrial radiation. The units of the input variables for each model were shown in the Appendix.

^a These two models were applied to monthly scale, while other models were applied to daily scale.

trends (with units of $\text{mm yr}^{-1} \text{yr}^{-1}$, i.e., mm yr^{-2}) to minimize the biases caused by timing of gaps within the data records (Donohue et al., 2010). Per-month and annual trends in AET and P were calculated in the same manner with PET.

Then, the hydroclimatological (i.e., water- or energy-limited) states could be defined based on the observed annual and per-month trends of AET and P , and the equivalent trends in PET would be hence obtained following the below criteria. That is, when the relationship between the trends of AET and P is positive (i.e., proportional), it should be defined as water-limited condition, and hence an inverse (i.e., complimentary) relationship would be expected between the trends of PET and AET. Alternatively, it should be regarded as the energy-limited environment, and a positive relationship would be expected between the trends of PET and AET.

3. Results

3.1. Assessing the magnitudes of PET

Prior to assessing PET dynamics, it is necessary to examine the reasonability of PET estimates in representing the magnitudes of

evaporative demand. Fig. 2 illustrates the relative magnitudes of different PET model estimates at particular ecosystems. Differences in the daily PET values estimated from different PET models were significant for all the eight sites (p -values < 0.05), and no models gave consistently low or high PET averages (Fig. 2). The coefficients of variance (CV_{PET}) among different PET model estimates tended to be smaller for the sites with higher precipitation (Table 3). The largest differences among PET estimates, with CV_{PET} up to 50%, occurred at the DX site where the maximum PET from the Linacre model (4.29 mm d^{-1}) was nearly six times the minimum from the Kharrufa model (0.78 mm d^{-1}) (Fig. 2g). For particular sites, some models gave PET estimates very different from the averages (Fig. 2). The Stephens-Steward model gave the smallest PET values except at the three alpine sites, and the Penman and Linacre models often gave higher values comparing with others (Fig. 2). The Thornthwaite and Kharrufa models generally gave high estimates for the hot climates of DHS and QYZ sites, but notably low for the alpine ecosystems (i.e., HBGC, HBSD and DX).

To evaluate the reasonability of PET models in representing the magnitudes of evaporative demand, we then compared different PET model estimates with the eddy-covariance AET data for specific sites. Results showed that the mean daily PET from all

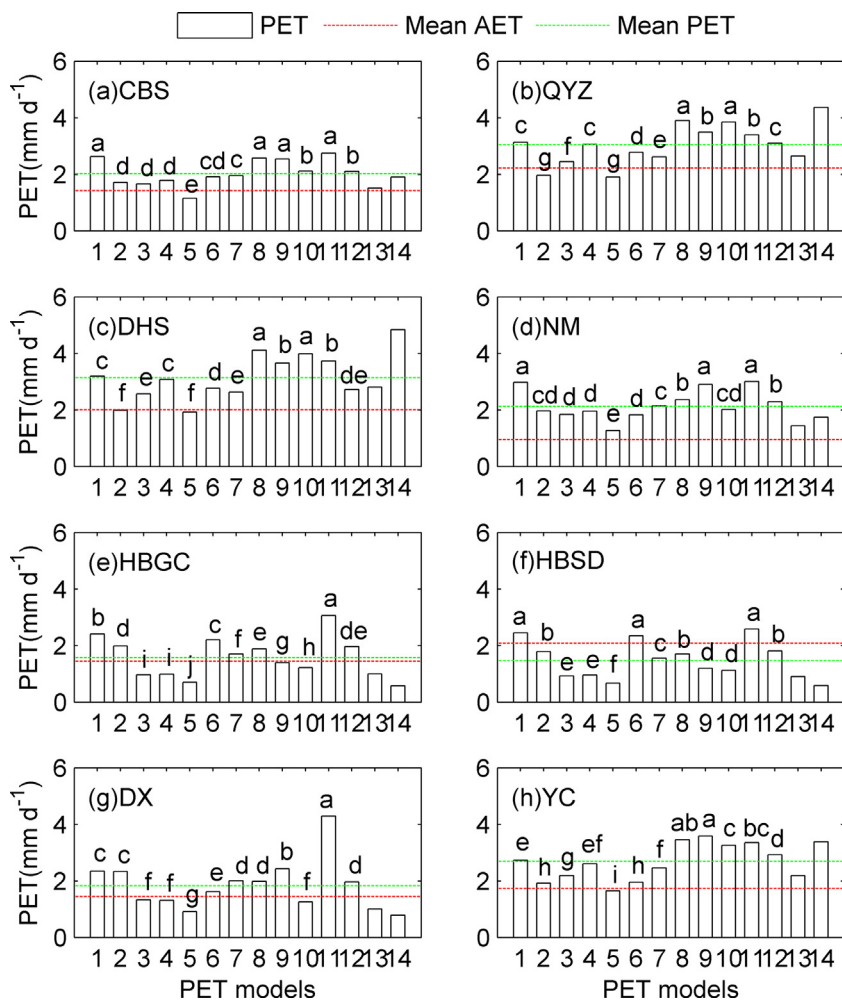


Fig. 2. Comparison of magnitudes of fourteen PET models estimates among different sites. Eight subplots indicate eight sites. The bars show the mean daily PET estimates during observational period for each model and site (Table 1). Different letters above bars within a subplot indicate significant differences among daily estimates of corresponding PET models based on Tukey's multiple comparison tests (without considering the Thornthwaite and Kharrufa models). For example, the first subplot indicates significantly different daily estimates between the first two PET models with p -value < 0.01 , while daily estimates of the sixth and seventh PET models are different at the level of p -value < 0.05 . For a given site, the green dashed lines indicate the averages of mean daily PET values estimated by fourteen PET models, while the red dashed lines indicate the mean daily AET values measured by eddy covariance method. The x-axis shows codes of PET models: 1-Penman, 2-Makkink, 3-Turc, 4-Jensen-Haise, 5-Stephens-Stewart, 6-Priestly-Taylor, 7-Hargreaves, 8-Balaney-Criddle, 9-Romanenko, 10-Hamon, 11-Linacre, 12-Hargreaves-Samani, 13-Thornthwaite, and 14-Kharrufa.

Table 3

Mean daily AET and PET values for different sites.

Sites	Mean AET (mm d ⁻¹) ^a	Mean PET (mm d ⁻¹) ^b	CV _{PET} ^c
CBS	1.41	2.02 ± 0.46	0.23
QYZ	2.22	3.04 ± 0.72	0.24
DHS	2.01	3.14 ± 0.83	0.27
NM	0.95	2.12 ± 0.54	0.25
HBGC	1.44	1.57 ± 0.72	0.46
HBSD	2.08	1.47 ± 0.66	0.45
DX	1.45	1.83 ± 0.90	0.49
YC	1.74	2.69 ± 0.65	0.24

^a These values are mean daily AET values measured by eddy covariance method.^b These values are averages of mean daily PET values estimated by fourteen PET models. The data after the plus and minus signs are the corresponding standard deviation.^c These values are coefficients of variance of mean daily PET values estimated by fourteen PET models for a given site.

the fourteen PET models were always larger than mean daily AET only at the NM site (Fig. 2d), while for the other sites around 30% of the models on average gave unreasonable PET estimates (i.e., PET < AET on average), especially that 11/14 of models gave unreasonable estimates at the HBSD site (Fig. 2). The robustness of PET models differed somewhat across the eight sites (Fig. 2). The Stephens-Steward model always gave smaller PET values than AET values except at the NM site. PET estimates from the Makkink model tended to be slightly lower than AET for sites with relatively sufficient water supply (i.e., DHS and QYZ). Besides, the Thornthwaite and Kharrufa models always yielded unreasonable PET estimates for the alpine ecosystems (Fig. 2e–g).

Overall, only three models selected in this study could produce reasonable magnitudes of evaporative demand (i.e., PET ≥ AET on

average) for all the eight sites, including the Penman, Priestly-Taylor and Linacre models, while the other 11 PET models have different degrees of inadequacies along with different ecosystems (Table 4).

3.2. Assessing the annual trends of PET

According to the results above, one fully physical (i.e., Penman), one radiation-based (i.e., Priestly-Taylor) and one temperature-based (i.e., Linacre) model were reasonable in representing the magnitudes of evaporative demand for all the eight sites (Table 4), which were further considered to assess their ability in reproducing annual and seasonal dynamics of evaporative demand.

At the annual time scale, we compared the annual trends in different PET estimates to those in AET and precipitation (*P*) for a given site (Table 5, column B). Take the DHS site for example, its annual trends in AET (−3.27 mm yr^{−2}) were in the opposite direction to *P* trends (78.48 mm yr^{−2}). Thus, DHS site is an energy-limited site at the annual time scale, and the annual trends of PET and AET should be at the same direction according to the proportional principle for the energy-limited areas. Table 5 indicates that all the three PET models have annual trends that are at the same direction with AET trends. As for the NM site, its annual trends in AET (9.76 mm yr^{−2}) were the same in direction with *P* trends (3.93 mm yr^{−2}), which makes NM a water-limited site at the annual time scale. Based on the complementary principle suitable for the water-limited areas, only the estimates of Penman and Linacre models displayed annual trends (−1.66 and −10.60 mm yr^{−2}, respectively) that are opposite in direction to AET trends (Table 5, column B).

Using the complementary or proportional principles applied to the NM and DHS sites, it could be concluded that the CBS, DHS and

Table 4

Reasonable PET models representing magnitudes of evaporative demand for different sites. Reasonable PET models refer to the models that give larger mean daily PET values than mean daily AET values according to the definition of PET (i.e., PET ≥ AET on average). The PET models with grey shadows are models which could give reasonable PET estimates for all the eight ecosystems.

PET model	CBS	QYZ	DHS	NM	HBGC	HBSD	DX	YC
Penman	√	√	√	√	√	√	√	√
Makkink	√			√	√		√	√
Turc	√	√	√	√				√
Jensen-Haise	√	√	√	√				√
Stephens-Steward				√				
Priestly-Taylor	√	√	√	√	√	√	√	√
Hargreaves	√	√	√	√	√		√	√
Blaney-Criddle	√	√	√	√	√		√	√
Romanenko	√	√	√	√			√	√
Hamon	√	√	√	√				√
Linacre	√	√	√	√	√	√	√	√
Hargreaves-Samani	√	√	√	√	√		√	√
Thornthwaite	√	√	√	√				√
Kharrufa	√	√	√	√				√

Table 5

Assessment on PET dynamics. Column A: annual-average estimates for three PET models. AET and precipitation values are also provided for reference. Column B: Annual trends for PET, AET and precipitation with *p*-values in brackets. Column C: Correlation coefficients between per-month trends in PET and equivalent trends in AET with *p*-values in brackets. See Table 1 for the observational periods for each site.

Site	PET model	A Annual-average rate (mm yr ⁻¹)	B Annual trend (mm yr ⁻²)	C Correlation with per-month AET trends
CBS	Penman	960.15	-2.86(0.74)	0.07(0.84)
	Priestly-Taylor	695.95	3.20(0.48)	0.05(0.87)
	Linacre	1000.70	-7.37(0.40)	0.02(0.95)
	Precipitation	736.51	22.62(0.35)	-0.11(0.73)
	AET	524.40	-3.91(0.34)	
QYZ	Penman	1143.22	-12.39(0.13)	-0.10(0.76)
	Priestly-Taylor	1014.11	-1.11(0.84)	0.31(0.33)
	Linacre	1239.69	-15.67(0.06)	-0.40(0.20)
	Precipitation	1363.74	34.28(0.30)	0.07(0.83)
	AET	809.62	13.14(0.33)	
DHS	Penman	1165.60	-15.10(0.24)	0.93(< 0.001)
	Priestly-Taylor	1008.26	-7.82(0.45)	0.89(< 0.001)
	Linacre	1364.23	-16.84(0.08)	0.73(0.01)
	Precipitation	1702.03	78.48(0.20)	-0.81(0.002)
	AET	733.21	-3.27(0.66)	
NM	Penman	1087.41	-1.66(0.81)	-0.23(0.48)
	Priestly-Taylor	668.70	7.98(0.22)	0.56(0.06)
	Linacre	1097.47	-10.60(0.11)	-0.42(0.17)
	Precipitation	289.00	3.93(0.74)	0.43(0.16)
	AET	347.51	9.76(0.18)	
HBGC	Penman	879.25	3.99(0.19)	0.47(0.12)
	Priestly-Taylor	805.95	2.05(0.33)	0.53(0.07)
	Linacre	1115.17	8.01(0.11)	0.24(0.44)
	Precipitation	500.60	-2.17(0.72)	-0.23(0.46)
	AET	526.88	-4.96(0.62)	
HBSD	Penman	1024.35	-56.29(0.04)	0.89(< 0.001)
	Priestly-Taylor	982.56	-74.69(0.04)	0.87(< 0.001)
	Linacre	1055.43	16.89(0.004)	0.32(0.31)
	Precipitation	490.73	-1.57(0.87)	-0.38(0.23)
	AET	760.22	-13.30(0.60)	
DX	Penman	980.73	5.24(0.42)	-0.31(0.33)
	Priestly-Taylor	654.38	-13.28(0.13)	0.18(0.57)
	Linacre	1852.93	40.16(0.08)	-0.52(0.09)
	Precipitation	451.17	-26.97(0.23)	0.74(0.01)
	AET	529.22	-1.53(0.92)	
YC	Penman	998.82	11.28(0.09)	0.60(0.04)
	Priestly-Taylor	714.71	3.92(0.43)	0.59(0.04)
	Linacre	1223.47	18.53(0.01)	0.23(0.46)
	Precipitation	639.63	-8.41(0.67)	-0.21(0.51)
	AET	633.88	10.22(0.01)	

YC sites were energy-limited sites at the annual time scale, and all the three PET models had annual trends that were at the same direction with AET trends except the Priestly-Taylor model at the CBS site (Table 5, column B). Meanwhile, the other five sites should be defined as water-limited sites. Results indicated that only the Penman and Linacre models reproduced annual trends that were opposite in direction to AET trends, whilst the Linacre model displayed a stronger degree of complementarity for the water-limited sites (Table 5, column B).

3.3. Assessing the per-month trends of PET

In order to assess the ability of the three PET models in capturing seasonal changes in evaporative demand, Table 5 compares the per-month trends (i.e., trend for Januaries, for Februaries, etc.) of each PET model estimates against the equivalent trends in AET and *P* for each site (Table 5, column C).

Results showed that, for the CBS, DHS, YC, HBGC and HBSD sites, the per-month trends in AET were inversely related to those in *P* with negative *R* values (Table 5, column C), which indicated that the changes in the seasonality of AET were mainly determined by

energy supply (i.e., energy-limited) at these five sites, and the per-month trends of AET and PET should follow the same direction. Table 5 indicates that all the three PET models have per-month trends that are at the same direction with the observed per-month trends in AET for the five sites, whilst the *R* values for the Penman and Priestly-Taylor models were similar in magnitudes but larger than that for the Linacre model (Table 5, column C).

Turning to the QYZ, NM and DX sites, the per-month trends in AET were positively related to those in *P* (Table 5, column C), which indicated that the per-month changes in AET were water-limited at these three sites. Based on the complementary principle, only the estimates of Penman and Linacre models had per-month trends that were inversely related to the observed per-month trends in AET for these sites, whilst a stronger degree of complementarity was observed for the Linacre model at each site (Table 5, column C).

The findings above were further demonstrated when the per-month trends were examined graphically (Fig. 3 and Fig. 4). According to the observed relationship between per-month trends of AET and *P*, Fig. 3 and Fig. 4 also show that there are seasonal switches between water- and energy-limited states for many sites.

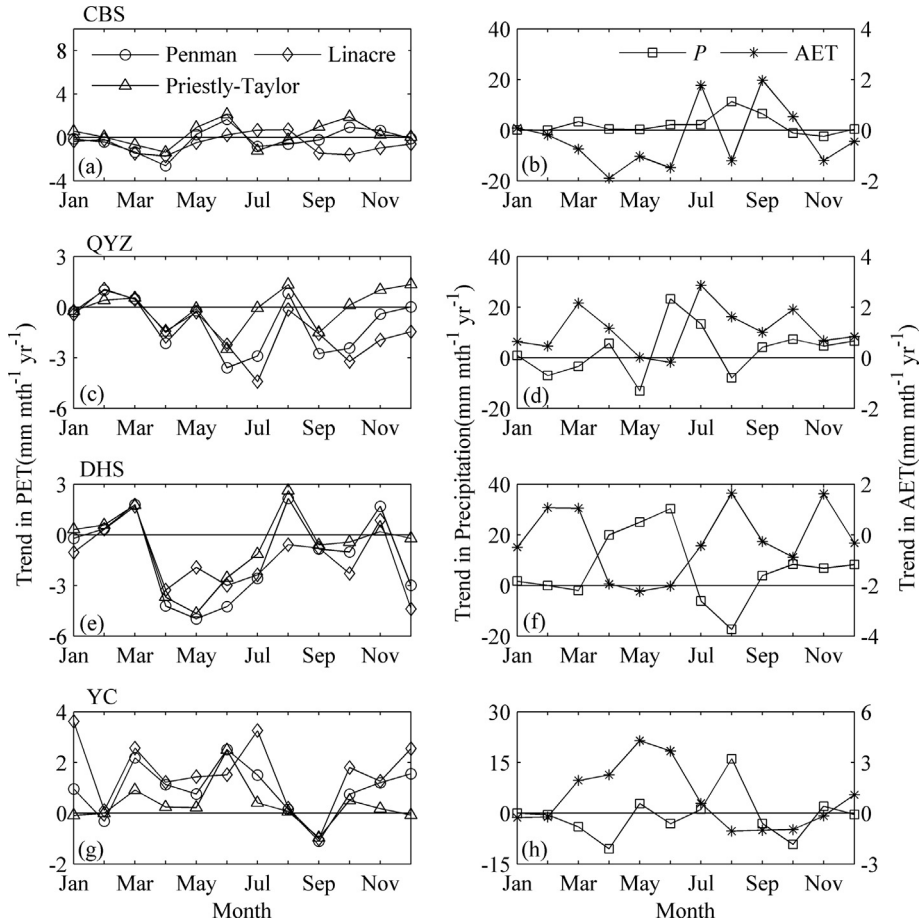


Fig. 3. Per-month trends in PET (left column), AET and precipitation (right column) for the three forest sites (i.e., CBS, QYZ and DHS) and cropland site (i.e., YC).

For example, at the CBS and NM sites, changes in AET basically followed PET trends during May to September, but mainly followed changes in P during other periods (Figs. 3b, 4b). That is, the hydroclimatological state at CBS and NM sites switched from water- to energy-limited state around May, and then turned around in September. Similarly, the hydroclimatological states for the QYZ site were mainly energy-limited during the first half year, but switched to water-limited states around July (Fig. 3d). Fig. 3 and Fig. 4 show that, the Linacre model was unable to capture the PET dynamics during June to July at the CBS (Fig. 3a, b), QYZ (Fig. 3c, d), YC (Fig. 3g, h) and NM sites (Fig. 4a, b). Although the DHS site was always under energy-limited conditions for a whole year, the Linacre model also failed to reproduce the expected PET dynamics during April to June (Fig. 3e, f).

4. Discussion

4.1. Assessment on PET magnitudes

Before assessing the ability of PET models in capturing long-term dynamics of evaporative demand, a critical requirement is the reasonability of PET estimates representing the magnitudes of evaporative demand. Results demonstrated that all the fourteen PET models studied here produced significantly different PET estimates for particular sites across a wide range of biomes and climate regimes (Fig. 2), which agreed with the previous studies for more limited areas or models (e.g., Federer et al., 1996; Fisher et al., 2011). Such differences should be attributed to the land surface characteristics, primarily water conditions. Our results

showed that differences in diverse PET estimates tended to be smaller for the sites with higher water supply (i.e., precipitation). This is because that the soil moisture conditions of the relatively wet sites seems closer to the 'well-watered' setting for PET estimation than that of dryer areas, which hence makes the PET differences smaller for sites with comparatively larger water supply. Thus, the finding that the largest differences in PET estimates occurred at the DX site could be on account of its low soil water content. In fact, the precipitation of the DX site is comparable to that of other alpine ecosystems (i.e., HBGC and HBSD), and is a little heavier than the precipitation at the temperate semi-arid steppe site (i.e., NM) (Table 2). However, due to the high altitude, strong solar radiation, intense surface evaporation and poor soil water holding capacity at the DX site (Shi et al., 2006), its soil moisture condition is much lower than that at the HBGC and HBSD sites, and even lower than that at the NM site for some years.

Conceptually, AET should never exceed PET at a long-term scale (Fisher et al., 2011). However, our results showed that not all the PET models are satisfying in representing the upper limit of AET and hence the magnitudes of evaporative demand (Fig. 2). The reasonability of PET models differed for a given site (Fig. 2 and Table 4). This is mainly resulted from the differences in model input variables and model structures. As we know, each PET model was designed against respective climate conditions which were expressed by its key input variables. The failure of one PET model for one site might mean that this PET model has certain flaws in describing main drivers of the local surface evaporation at this site.

Take for example the case of Thornthwaite and Kharrufa models which generally underestimate PET of alpine ecosystems (Fig. 2).

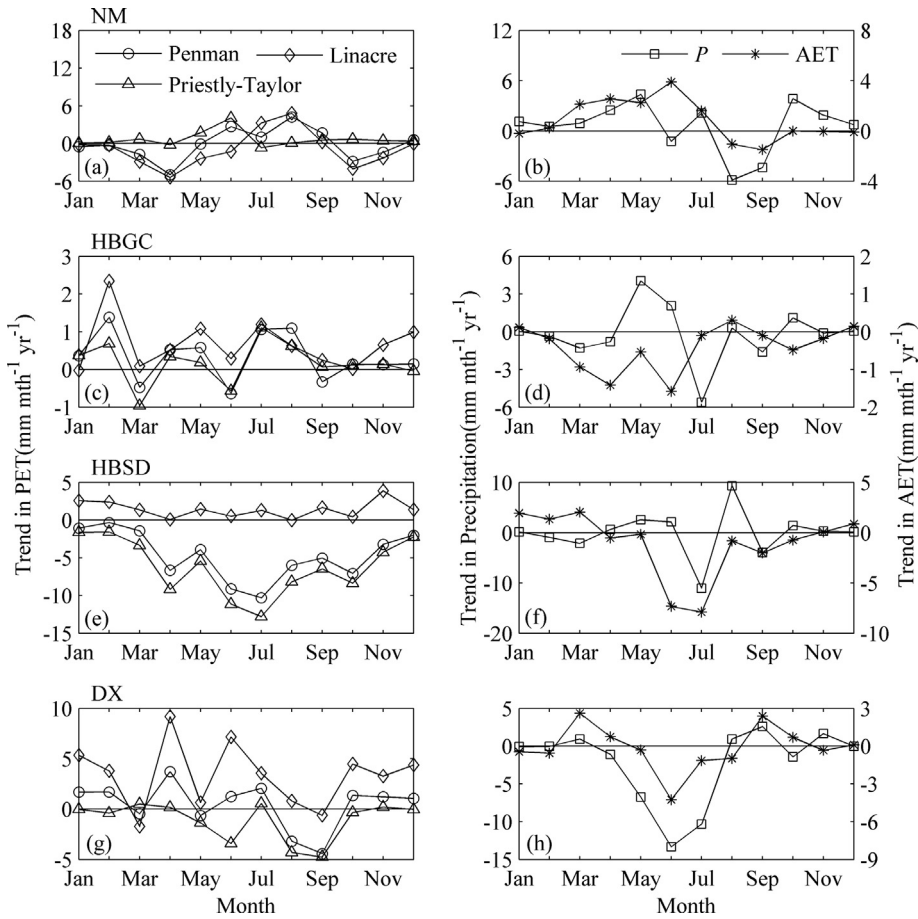


Fig. 4. Per-month trends in PET (left column), AET and precipitation (right column) for the three grassland sites (i.e., NM, HBGC, DX) and alpine wetland site (i.e., HBSD).

The mean air temperature of alpine ecosystems is considerably low, but their precipitation and especially solar radiation is quite abundant (Table 2). Zhang (1991) documented that the multi-mean annual precipitation of the HBGC and HBSD sites is about 50 mm higher than that over the northern China. As only air temperature is considered within the Thornthwaite and Kharrufa models, these two models thus seriously underestimate the strength of evaporative demand for the three alpine sites (Fig. 2).

However, pronounced differences still may appear among some PET models with same inputs variables and similar model structures, which should attribute to the differences in model parameters/coefficients. For example, the Stephens-Steward model has similar model structure with that of the Hargreaves and Jensen-Haise models, but their corresponding model coefficients are distinct (Appendix), which hence makes the Stephens-Steward model always produce smaller PET values than the latter two, and thereby makes its PET estimates smaller than AET observations for a majority of sites in this study (Fig. 2).

4.2. Assessment on PET dynamics

Given the above conclusions on the PET magnitudes, the Penman, Priestly-Taylor and Linacre models were found to be reasonable in representing the magnitudes of evaporative demand for all the eight sites across large gradients in climatic and vegetation conditions (Table 4). We then conducted the assessment on PET dynamics using these three PET models. As it happens, these three PET models were different in both model structures and main driving variables, comprising one fully physical, one radiation-based

and one temperature-based model (Table 2 and Appendix). Results showed that these three PET models produced obvious different estimates in both rates and trends for a given site (Table 5), which further manifested the necessity of this PET model assessment.

As we know, PET dynamics are primarily driven by four key meteorological variables (i.e., net radiation, vapor pressure deficit, wind speed and air temperature), which have been physically involved in the Penman model (Penman, 1948). As to the Linacre model, this temperature-based method was simplified from the Penman equation and incorporates the effects of elevation, latitude and dewpoint temperature (Linacre, 1977). Thus, the influences of vapor pressure on PET could also be reflected in the Linacre model, as dewpoint temperature is the temperature when the actual vapor pressure is the saturation vapor pressure (Allen et al., 1998). Hence, our findings demonstrated that the Penman and Linacre models could faithfully reproduce the 'realistic' dynamics in evaporative demand for both water- and energy-limited environments at both long-term annual and seasonal scales (Table 5). However, the Priestly-Taylor model does not take the contribution of vapor pressure (deficit) into account and generally refers to evaporation from wet surfaces (Priestley and Taylor, 1972). Therefore, the Priestly-Taylor model usually failed in capturing dynamics in evaporative demand under water-limited conditions at different time scales (Table 5), and the radiation-based PET models are best suitable for the energy-limited environments.

According to the observed relationships between per-month trends of AET and P , we found that there often existed seasonal switches between water- and energy-limited states for many sites (Fig. 3 and Fig. 4). And, it is also one important aspect for a PET

model to capture the seasonal dynamics of evaporative demand during transition stages between water- and energy-limited states. For the CBS, QYZ, YC and NM sites, our results indicated that the Linacre model failed to reproduce the expected PET dynamics during June to July (Fig. 3 and Fig. 4) when the soil moisture content was supposed to increase due to the carry-over effects of increased rainfall amount (around May) on soil moisture content (Guo et al., 2012). It might be because that the changes in air temperature followed the increases in soil water availability are not as sensitive as net radiation and vapor pressure (deficit), which hence makes the Linacre model unable to reproduce the dynamics in evaporative demand during transition stages at these sites. As to the DHS site, the whole year could be divided into wet season (from April to September) and dry season (from October to March in the next year), although the DHS site is always under energy-limited conditions (Fig. 3e, f). Thus, the rainfall and soil moisture content would increase around April at the DHS site, which hence explains why the Linacre model failed to reproduce the expected PET dynamics during April to June at the DHS site (Fig. 3e).

5. Conclusion

Fourteen PET models were considered in this study to assess their ability in representing the magnitudes and long-term (typically 2003–2011) dynamics of atmospheric evaporative demand at eight ecosystems across various biomes and climatic regimes in China. Results indicated that only three PET models could produce reasonable magnitudes of evaporative demand (i.e., $PET \geq AET$ on average) for all the eight sites, including the: (i) Penman; (ii) Priestly-Taylor and (iii) Linacre models. And, nearly all these three PET models could faithfully reproduce the dynamics in evaporative demand for the energy-limited conditions at both annual and seasonal scales, while only the Penman and Linacre models could represent dynamics in evaporative demand for the water-limited conditions. However, the Linacre model was unable to reproduce the seasonal switches between water- and energy-limited states for some sites.

The findings reported in this research demonstrate that the choice of PET models will be essential in the evaporative demand modeling efforts and other applications. The so many failures of PET models in representing the magnitudes and dynamics of evaporative demand also confirm that some PET models have limited validity. Therefore, to ensure the correctness of results, we should either choose the reasonable ones or conduct local calibrations for the studied areas. The reasonable PET models representing the magnitudes and dynamics of evaporative demand for different sites studied here have been elected in this paper. However, it should be clear that different results may emerge from alternative PET models and biome types. This China-setting study aimed to highlight the potential problems with respect to PET-related researches, and draw more studies on the evaluation of PET models over more biome types worldwide.

Acknowledgements

This work was financially supported by National Natural Science Foundation of China (Grant NO. 31290221, 31420103917), and National Key Research and Development Program of China (NO. 2016YFA0600104, 2016YFA0600103). We acknowledge all the PIs and researchers of ChinaFLUX sites for contributing valuable data. We acknowledge the database and technical support from Chinese Ecosystem Research Network and Oak Ridge National Laboratory. We also gratefully thank the editors and reviewers for spending their valuable time and providing constructive comments.

Appendix A. Supplementary data

Supplementary data associated with this article can be found, in the online version, at <http://dx.doi.org/10.1016/j.jhydrol.2017.05.056>.

References

- Allen, R.G., Pereira, L.S., Raes, D., Smith, M., 1998. Crop evapotranspiration—Guidelines for computing crop water requirements, FAO Irrigation and Drainage Paper No. 56. FAO, Rome.
- Brümmer, C. et al., 2012. How climate and vegetation type influence evapotranspiration and water use efficiency in Canadian forest, peatland and grassland ecosystems. *Agric. For. Meteorol.* 153, 14–30.
- Brutsaert, W., Parlange, M.B., 1998. Hydrologic cycle explains the evaporation paradox. *Nature* 396 (6706), 30.
- Budyko, M.I., 1978. The heat balance of the earth's surface. Gidrometeoizdat, leningrad.
- Donohue, R.J., Roderick, M.L., McVicar, T.R., 2007. On the importance of including vegetation dynamics in Budyko's hydrological model. *Hydrol. Earth Syst. Sci.* 11 (2), 983–995.
- Donohue, R.J., McVicar, T.R., Roderick, M.L., 2010. Assessing the ability of potential evaporation formulations to capture the dynamics in evaporative demand within a changing climate. *J. Hydrol.* 386 (1–4), 186–197.
- Federer, C.A., Vörösmarty, C., Fekete, B., 1996. Intercomparison of methods for calculating potential evaporation in regional and global water balance models. *Water Resour. Res.* 32 (7), 2315–2321.
- Finnigan, J.J., Clement, R., Malhi, Y., Leuning, R., Cleugh, H.A., 2003. A re-evaluation of long-term flux measurement techniques—Part I: Averaging and coordinate rotation. *Bound-Layer Meteorol.* 107 (1), 1–48.
- Fisher, J.B., DeBiase, T.A., Qi, Y., Xu, M., Goldstein, A.H., 2005. Evapotranspiration models compared on a Sierra Nevada forest ecosystem. *Environ. Modell. Software* 20 (6), 783–796.
- Fisher, J.B., Whittaker, R.J., Malhi, Y., 2011. ET come home: potential evapotranspiration in geographical ecology. *Glob. Ecol. Biogeogr.* 20 (1), 1–18.
- Guo, Q. et al., 2012. Spatial variations in aboveground net primary productivity along a climate gradient in Eurasian temperate grassland: effects of mean annual precipitation and its seasonal distribution. *Glob. Change Biol.* 18 (12), 3624–3631.
- Hamon, W.R., 1960. Estimating potential evapotranspiration Bachelor dissertation Thesis. Massachusetts Institute of Technology, USA.
- Hao, Y.B. et al., 2007. Seasonal and interannual variation in water vapor and energy exchange over a typical steppe in Inner Mongolia, China. *Agric. Forest Meteorol.* 146 (1–2), 57–69.
- Hargreaves, G.H., 1975. Moisture availability and crop production. *Transac. ASAE.* 18 (5), 980–984.
- Hargreaves, G.H., Samani, Z.A., 1982. Estimating potential evapotranspiration. *J. Irrig. Drain. Div.* 108 (3), 225–230.
- Hobbins, M., Wood, A., Streubel, D., Werner, K., 2012. What drives the variability of evaporative demand across the conterminous United States? *J. Hydrometeorol.* 13 (4), 1195–1214.
- Jensen, M.E., Haise, H.R., 1963. Estimating evapotranspiration from solar radiation. *Proc. Am. Soc. Civil Eng. J. Irrig. Drain. Div.* 89, 15–41.
- Linacre, E.T., 1977. A simple formula for estimating evaporation rates in various climates, using temperature data alone. *Agric. Meteorol.* 18 (6), 409–424.
- Liu, W.B., Sun, F.B., 2016. Assessing estimates of evaporative demand in climate models using observed pan evaporation over China. *J. Geophys. Res. Atmos.* 121, 8329–8349.
- Lu, J.B., Sun, G., McNulty, S.G., Amatya, D.M., 2005. A comparison of six potential evapotranspiration methods for regional use in the southeastern United States. *J. Am. Water Resour. Assoc.* 41 (3), 621–633.
- McGuinness, J.L., Bordne, E.F., 1972. A comparison of lysimeter-derived potential evapotranspiration with computed values. US Dept. of Agriculture.
- McVicar, T.R. et al., 2012a. Global review and synthesis of trends in observed terrestrial near-surface wind speeds: Implications for evaporation. *J. Hydrol.* 416–417, 182–205.
- McVicar, T.R., Roderick, M.L., Donohue, R.J., Van Niel, T.G., 2012b. Less bluster ahead? Ecohydrological implications of global trends of terrestrial near-surface wind speeds. *Ecohydrology* 5 (4), 381–388.
- Oak Ridge National Laboratory Distributed Active Archive Center (ORNL DAAC), 2015. MODIS subsetted land products, Collection 5. Available on-line [<http://daac.ornl.gov/MODIS/modis.html>] from ORNL DAAC, Oak Ridge, Tennessee, U.S.A. Accessed February 27, 2015.
- Oki, T., Kanae, S., 2006. Global hydrological cycles and world water resources. *Science* 313 (5790), 1068–1072.
- Oudin, L. et al., 2005. Which potential evapotranspiration input for a lumped rainfall-runoff model?: Part 2—Towards a simple and efficient potential evapotranspiration model for rainfall-runoff modelling. *J. Hydrol.* 303 (1), 290–306.
- Penman, H.L., 1948. Natural evaporation from open water, bare soil and grass. *Proc. R. Soc. Lond. A* 193 (1032), 120–145.
- Priestley, C.H.B., Taylor, R.J., 1972. On the assessment of surface heat flux and evaporation using large-scale parameters. *Mon. Weather Rev.* 100 (2), 81–92.

- Rao, L.Y., Sun, G., Ford, C.R., Vose, J.M., 2011. Modeling potential evapotranspiration of two forested watersheds in the southern Appalachians. *Trans. ASABE* 54 (6), 2067–2078.
- Reichstein, M. et al., 2005. On the separation of net ecosystem exchange into assimilation and ecosystem respiration: review and improved algorithm. *Glob. Change Biol.* 11 (9), 1424–1439.
- Robinson, E.L., Blyth, E.M., Clark, D.B., Finch, J., Rudd, A.C., 2017. Trends in atmospheric evaporative demand in Great Britain using high-resolution meteorological data. *Hydrol. Earth Syst. Sci.* 21 (2), 1189–1224.
- Roderick, M.L., Farquhar, G.D., 2004. Changes in Australian pan evaporation from 1970 to 2002. *Int. J. Climatol.* 24 (9), 1077–1090.
- Romanenko, V.A., 1961. Computation of the autumn soil moisture using a universal relationship for a large area, Proceedings. Ukrainian Hydrometeorological Research Institute, Ukrainian.
- Shi, P.L. et al., 2006. Net ecosystem CO₂ exchange and controlling factors in a steppe-Kobresia meadow on the Tibetan Plateau. *Sci. China, Ser. D Earth Sci.* 49 (S2), 207–218.
- Song, Y., Ryu, Y., Jeon, S., 2014. Interannual variability of regional evapotranspiration under precipitation extremes: A case study of the Younisan River basin in Korea. *J. Hydrol.* 519, 3531–3540.
- Thornthwaite, C.W., 1948. An approach toward a rational classification of climate. *Geogr. Rev.* 38 (1), 55–94.
- Wang, K.C., Dickinson, R.E., Liang, S., 2012. Global atmospheric evaporative demand over land from 1973 to 2008. *J. Clim.* 25 (23), 8353–8361.
- Webb, E.K., Pearman, G.I., Leuning, R., 1980. Correction of flux measurements for density effects due to heat and water vapour transfer. *Q. J. R. Meteorol. Soc.* 106 (447), 85–100.
- Wen, X.F. et al., 2006. Soil moisture effect on the temperature dependence of ecosystem respiration in a subtropical *Pinus* plantation of southeastern China. *Agric. For. Meteorol.* 137 (3–4), 166–175.
- Xu, C.Y., Singh, V.P., 2000. Evaluation and generalization of radiation-based methods for calculating evaporation. *Hydrol. Process.* 14 (2), 339–349.
- Xu, C.Y., Singh, V.P., 2001. Evaluation and generalization of temperature-based methods for calculating evaporation. *Hydrol. Process.* 15 (2), 305–319.
- Xu, C.Y., Singh, V.P., 2002. Cross comparison of empirical equations for calculating potential evapotranspiration with data from Switzerland. *Water Resour. Manage.* 16 (3), 197–219.
- Yang, D.W., Sun, F.B., Liu, Z.Y., Cong, Z.T., Lei, Z.D., 2006. Interpreting the complementary relationship in non-humid environments based on the Budyko and Penman hypotheses. *Geophys. Res. Lett.* 33 (18), L18402.
- Yu, G.R. et al., 2006. Overview of ChinaFLUX and evaluation of its eddy covariance measurement. *Agric. For. Meteorol.* 137 (3), 125–137.
- Yu, G.R. et al., 2013. Spatial patterns and climate drivers of carbon fluxes in terrestrial ecosystems of China. *Glob. Change Biol.* 19 (3), 798–810.
- Zhang, J., 1991. A Series of Climate for China. China Meteorological Press, Beijing (in Chinese).
- Zhang, J.H., Han, S.J., Yu, G.R., 2006. Seasonal variation in carbon dioxide exchange over a 200-year-old Chinese broad-leaved Korean pine mixed forest. *Agric. For. Meteorol.* 137 (3–4), 150–165.
- Zhao, F.H. et al., 2007. Canopy water use efficiency of winter wheat in the North China Plain. *Agric. Water Manage.* 93 (3), 99–108.
- Zheng, H., Wang, Q.F., Zhu, X.J., Li, Y.N., Yu, G.R., 2014. Hysteresis responses of evapotranspiration to meteorological factors at a diel timescale: patterns and causes. *PLoS One* 9 (6), e98857.
- Zhu, Z.L. et al., 2005. Correcting method of eddy covariance fluxes over non-flat surfaces and its application in ChinaFLUX. *Sci. China Ser. D-Earth Sci.* 48, 42–50.